Bijok, Nicolaus; Fiskari, Juha; Gustafson, Richard R.; Alopaeus, Ville

Modelling the kraft pulping process on a fibre scale by considering the intrinsic heterogeneous nature of the lignocellulosic feedstock

Published in:
Chemical Engineering Journal

DOI:
10.1016/j.cej.2022.135548

Published: 15/06/2022

Document Version
Publisher's PDF, also known as Version of record

Chemical Engineering Journal 438 (2022) 135548

Contents lists available at ScienceDirect

Chemical Engineering Journal

journal homepage: www.elsevier.com/locate/cej

Modelling the kraft pulping process on a fibre scale by considering the intrinsic heterogeneous nature of the lignocellulosic feedstock

Nicolaus Bijok [a,*], Juha Fiskari [b], Richard R. Gustafson [c], Ville Alopaeus [a,b]

[a] Department of Chemical and metallurgical engineering, School of Chemical Technology, Aalto University, PO Box 16100, FI-00076 Aalto, Finland
[b] Fibre Science and Communication Network (FSCN), Mid Sweden University, Holmgatan 10, SE-85170 Sundsvall, Sweden
[c] University of Washington, School of Environmental and Forest Sciences, Biofuels and Bioproducts Laboratory, Box 352100, Seattle, WA, 98195-2100, US

ARTICLE INFO

Keywords:
Chemical pulp
Uniformity
Kappa number
Digester
Distribution
Lignin reactivity

ABSTRACT

Renewable raw materials such as lignocellulose are inherently complex and demanding in chemical processing compared to petroleum-based feedstocks. This article addresses the challenge of developing a general model framework for modelling lignocellulosic feedstock on a fibre scale, considering its inherent heterogeneous nature in terms of the fundamental chemical component distribution in addition to its anisotropic structural properties. The presented model is tested and validated for the well-established kraft pulping process. Simulations and parameter estimation are carried out to investigate the kappa number distribution of softwood fibres during kraft pulping by using experimental data from the literature showing non-uniform delignification. A moving grid discretisation method for the distributed concentration variables is used to predict the reaction of the wood solids. The results suggest that an inherent fundamental chemical component distribution can be hypothesised as one source of the non-uniform delignification. The model indicates that a Gaussian distribution can be assumed for the initial lignin concentration within softwood. In addition, an investigation of the lignin kinetics suggests that the reactivity of lignin during kraft pulping decreases as the delignification progresses.

1. Introduction

Modelling and simulation are powerful tools for the development and optimisation of chemical processes. In the field of petroleum-based processes, computational models are well established and experience great reliability. However, with the ongoing shift towards a sustainable economy, these feedstocks will gradually be substituted with renewable raw materials such as lignocellulosic feedstocks. This transition comes with the challenge of handling the hierarchical complex and inherent variable lignocellulose, which demands sophisticated modelling approaches on different scales [1]. Understanding the nature and variability of the biomass raw material is crucial for process development to maintain uniform product quality and sufficiently low production costs. Properties of the feedstock such as chemical composition, structural differences and initial feedstock quality might vary even within the same feedstock species and must be addressed during model development [2].

The pulp and paper industry is the world's largest producer of bioenergy and biomaterials, with the kraft pulping technology as its predominating pulping process. The traditional kraft process aims to produce paper pulp. However, the process offers opportunities to integrate biorefinery concepts into existing kraft pulp mills, making the overall process more efficient and profitable [3]. The main objective of this chemical pulping process is the delignification of wood into cellulose fibres by simultaneously minimising carbohydrate losses. The cooking liquor mixture of sodium hydroxide and sodium sulfide with its active cooking species hydroxide and hydrogen sulfide ions react at elevated temperatures with the solids of the porous wood chips inside a batch or continuous digester configuration [4]. It is a well-established technology with a broad knowledge ranging from laboratory scale tests to industrial operations. Despite its long and successful history, there are still relatively few rigorous modelling efforts considering intrinsic mass transfer and reaction together with the inherent heterogeneous nature of the biomass feedstock. On the other hand, the mature state of the technology opens opportunities to build and validate mathematical models capable of scaling up the kraft process and related biorefinery operations that share many similar characteristics.

The utilised feedstock for the kraft pulping process is wood, which can be divided into softwood and hardwood, with even more different species within each group. Macroscopic structures of the porous interior and average chemical compositions might differ depending on the

* Corresponding author.
E-mail address: nicolaus.bijok@aalto.fi (N. Bijok).

https://doi.org/10.1016/j.cej.2022.135548
Received 10 January 2022; Received in revised form 23 February 2022; Accepted 26 February 2022
Available online 1 March 2022

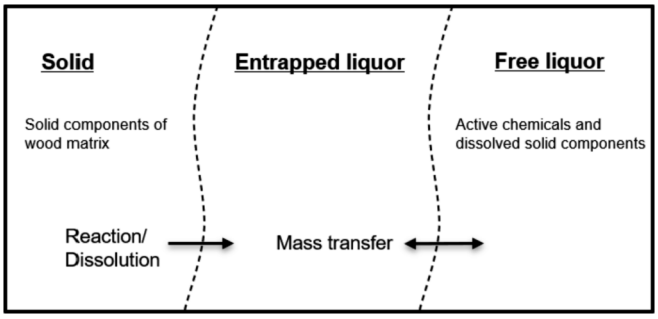

Fig. 1. Schematic illustration of the three phases within the digester.

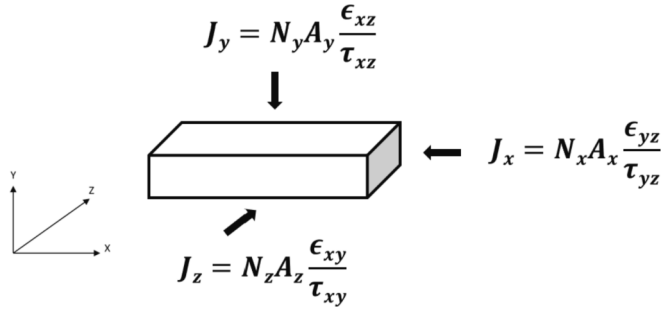

Fig. 2. Schematic illustration of the wood chip with the directional and structural dependent fluxes in each direction.

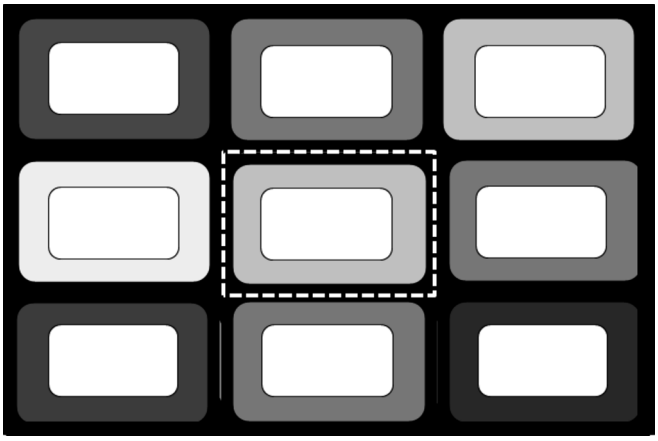

Fig. 3. Schematical illustration of the wood fibres arrangement within the wood and the boundary definition for one fibre in the context of the present mathematical model. The grey shades represent different concentrations of, e. g., lignin. (high lignin = black, low lignin = white).

species. The fundamental chemical components of wood are mainly lignin, cellulose, and hemicellulose, organised in a fibre with several layers, the secondary wall, primary wall, and middle lamella [5]. The middle lamella surrounds the fibre cell and holds the neighbouring fibres together in cell corners which are high in lignin, whereas the secondary wall layers comprise most carbohydrates [6–8]. Raman images show that the fundamental chemical components are distributed into these morphological regions and can vary across one distinct region [9]. Despite the knowledge of the distributed character of the fundamental chemical components, classical models aim to predict the delignification of wood on an average basis.

One such model family was developed at Purdue University. The models describe the fractionation process with a kinetic model distinguishing the solids of wood into five different components reacting in parallel, where some have an unreactive and/or slow/fast reactive fraction. Diffusion of the active inorganic chemicals is modelled as ideal mixed within the wood chip. [10–12]

Another approach to model kraft pulping is the University of Washington model. Here the kinetics are given for lignin and carbohydrates in three subsequent phases. The diffusion of hydroxide and hydrogen sulfide ions is modelled one-directional. [13,14]

Both approaches have limited considerations regarding the heterogeneous nature of the wood, especially the distribution of the chemical components is neglected. Lately, some theoretical models have been proposed to take the anisotropic nature of the wood chip into account [15–18]. These studies mainly focus on the heterogeneous mass transfer phenomena and the resulting non-uniform delignification. However, also neglect the intrinsic chemical distribution within the wood.

The issue of non-uniform delignification was addressed by Ming regarding the kappa number distribution of kraft pulps [19]. In that study, pulping experiments with softwood were conducted and evaluated in the light of fibre scale uniformity. The kappa number, which is an indication of the pulp's residual lignin content, was measured for several pulping conditions and wood chip sizes. The results have confirmed that process conditions and chip sizes impact the kappa number variability due to diffusion limitations. Moreover, the results have shown that intrinsic fibre scale heterogeneity exists, independent of other pulping parameters. The author developed a model to account for the intrinsic fibre scale non-uniformity by using the model structure of the Washington University model family to predict the kappa number and impose a Gaussian distribution on the average kappa number. Such a post-process accounts for the heterogeneity of the fractionation process but does not explain the origin of the inherent raw material character. The author pointed out that kappa number variability has consequences for downstream unit operations and pulp properties, such as bleaching and pulp strength [20–22]. Therefore, it must be addressed in any consideration regarding process optimisation.

This work proposes a novel approach for modelling the kraft pulping process by considering the distributed character of the fundamental chemical components within the wood chip and the resulting non-uniform delignification on a fibre level. Moreover, the three-dimensional properties of the anisotropic raw material structure within the porous wood are considered. The kinetic and diffusion parameters can be obtained from available literature models and incorporated into the model framework.

2. Model hypotheses and equations

A batch reactor framework for modelling anisotropic porous biomass is developed to account for the delignification of wood, which includes three phases in the digester (Fig. 1). The reaction site between the solid wood matrix and active chemicals appears at the interface between the solid and entrapped liquor phases. The dissolved solids and active chemicals prevail in the porous structure of the wood and are in mass transfer with the free liquor phase in the digester.

The solid and entrapped liquor phase combined represent the wood chip. An illustration of the chip with the structural and diffusional differences in each direction is shown in Fig. 2.

The total mass transfer of active chemicals into the chips is the sum of the contributions from each site, respectively. The wood chip is built-up of wood fibres arranged in an array with $p_{fraction}$ of fibres have a specific initial composition of lignin and carbohydrates to consider the heterogeneous character of the wood in terms of concentration variability. Fig. 3 shows the schematic arrangement of nine fibres with different initial compositions and the boundary definition for one fibre in the context of the present mathematical model. No distinction between the morphological regions of the fibre is made at this stage. The model describes the fibre concentration as an average concentration, including the secondary wall, the middle lamella, and the cell corner portion for one distinct fibre.

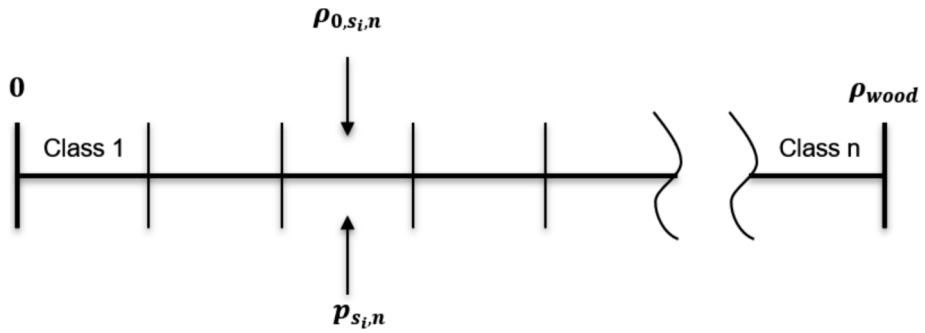

Fig. 4. Discretisation of a solid component mass concentration into n arbitrary concentration classes.

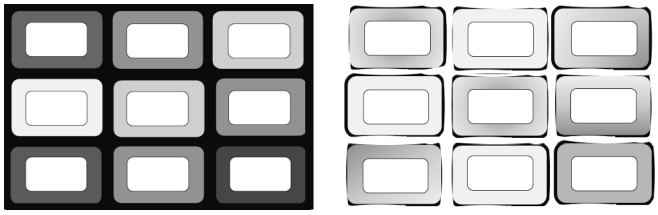

Fig. 5. Schematical illustration of the delignification process of individual fibres. The initial state of the fibres with the distributed fundamental chemical component concentrations (left). State of the individual fibres after delignification (right). The grey shades represent different concentrations (high = black, low = white).

Solid-phase mass balance for the wood fibres

The fibre component mass balances describe the amount of each fundamental chemical component in kg per control volume of fibre. Due to the heterogeneous character of the wood, these mass concentrations are assumed to be distributed variables. When a large number of fibres are analysed, these concentrations vary from fibre to fibre. In order to describe this variability, the density distributions are discretised into separate concentration classes. Untreated fibre concentrations are first allocated to these classes according to the raw material properties. Arbitrary distributions can be assumed for each initial concentration of the solid components. Although the concentration for each fundamental chemical component might vary independently, only one coordinate is selected for the present model analysis to keep the model manageable. The most relevant distributed concentration concerning pulping is lignin. At the same time, the other fundamental chemical components are assumed to be distributed so that the overall mass density is constant in the solid wood matrix. This assumption can be relaxed if needed since the one-dimensional density distribution assumes a pre-defined relationship between densities of all fundamental chemical components.

The continuous concentration distributions are discretised into n equal concentration classes ranging from zero to the density of the considered wood species, as is shown in Fig. 4. The upper and lower concentration limits define the initial mass concentration for a solid component in each class:

$$\rho_{0,s_i,n} = \frac{\rho_{max_{0,s_i,n}} + \rho_{min_{0,s_i,n}}}{2} \tag{1}$$

During the reaction, the material is not moved from one class to another, but the concentration in each class varies according to the predicted rate. This method corresponds to a moving grid technique for the discretisation of distributed variables. Such an approach reduces numerical diffusion inherent to class-to-class material transfer in typical numerical schemes for convection.

Upon pulping, the concentration in each class is followed based on the reaction rate according to:

$$\frac{d\left(\rho_{s_i,n} V_{fibre}\right)}{dt} = R_{s_i,n} V_{fibre} \tag{2}$$

Where the solid component s_i of the fibre reacts according to its reaction rate $R_{s_i,n}$ within each concentration class n. A total solid reaction rate is calculated, where the individual reaction rates $R_{s_i,n}$ of the respective fibre concentration classes are weighted by the fraction of fibres $p_{s_i,n}$ within the class n and are summed up to the total reaction rate of the solid component s_i in the wood chip:

$$R_{total,s_i} = \sum_{n=1}^{n} R_{s_i,n} p_{s_i,n} \tag{3}$$

Fig. 5 illustrates the solid phase delignification process for the individual fibres. The left side shows the initial state and concentration distribution of the fundamental chemical components within the fibres, whereas the right side illustrates the situation after the delignification process.

Entrapped liquor phase mass balance for the wood chip

Mass balances of the entrapped liquor phase account for the liquid components within the porous system of the wood chip, reacting with the solid components of the fibre:

$$\frac{d\left(\rho_{e_j} V_e\right)}{dt} = 2\left[\left(N_{j_x} A_{yz} \frac{\varepsilon_{yz}}{\tau_{yz}}\right) + \left(N_{j_y} A_{xz} \frac{\varepsilon_{xz}}{\tau_{xz}}\right) + \left(N_{j_z} A_{xy} \frac{\varepsilon_{xy}}{\tau_{xy}}\right)\right] + n_{fibers} V_{fibre} R_{e_j} \tag{4}$$

where $N_{j_{direction}} A_{direction}$ refers to the mass transfer in or out of the chip through the surface of the respective direction and R_{e_j} denotes to the reaction rate of the e_j liquid component. The structural differences of the anisotropic wood chip are considered with the porosity to tortuosity ratio $\frac{\epsilon_{direction}}{\tau_{direction}}$ throughout each direction. The flux between the free and entrapped liquor is described by:

$$N_{j_{direction}} = K_{ol,j_{direction}} \left(\rho_{f_j} - \rho_{e_j}\right) \tag{5}$$

where $K_{ol\,j_{direction}}$ refers to an overall mass transfer coefficient, including the external film and internal diffusion resistances between the bulk phase and the chip centre of the respective direction. The reaction rates of the entrapped liquid components are related to the reaction rates of the solid components through a stoichiometric coefficient matrix:

$$R_{e_j} = \sum_{l=1}^{l} b_{j,l} R_{total,s_l} \tag{6}$$

Here the stoichiometric coefficient matrix contains the relationship between the quantities of the solid components and the active chemical reactants. The total consumption of the active chemicals results from the total reaction rate sum of the solid components involved with the reactants.

Free liquor phase mass balance for the digester

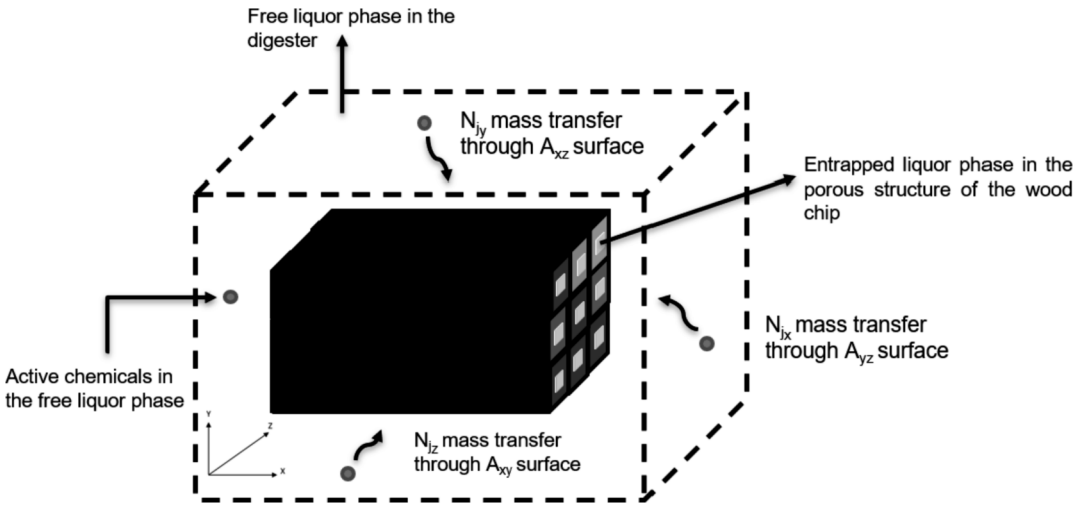

Fig. 6. Schematical illustration of the three-phase mass balances, solid and entrapped liquor phase (wood chip), and surrounding free liquor phase in the digester (dashed lined box).

Table 1
Overview of the cooking experiments and the fibre kappa number distribution statistics [19].

Pulp ID	Effective alkali [g/L]	Cooking time [h]	Kappa number distribution			
			Average [-]	Standard Deviation [-]	Coefficient of Variation [-]	Skewness [-]
EW01	40	18	76.5	11.3	0.15	0.094
EW02	40	24	56.7	9.28	0.16	0.071
EW03	40	36	36.8	5.91	0.16	0.089
EW04	40	46	26.1	4.32	0.17	−0.016
HA01	160	7	39.6	6.41	0.16	0.069
HA02	160	9	22.2	3.64	0.16	−0.036

The free liquor phase contains the same liquid components as the entrapped liquor phase. The mass balance is presented as:

$$\frac{d\left(\rho_{fj} V_f\right)}{dt} = -2n_{chips}\left(N_{j_x} A_{yz}\frac{\varepsilon_{yz}}{\tau_{yz}} + N_{j_y} A_{xz}\frac{\varepsilon_{xz}}{\tau_{xz}} + N_{j_z} A_{xy}\frac{\varepsilon_{xy}}{\tau_{xy}}\right) \tag{7}$$

Where V_f is the free liquor volume of the digester and $N_{j_{direction}} A_{direction}\frac{\varepsilon_{direction}}{\tau_{direction}}$ describes the flux from the free liquor to the entrapped liquor phase of the wood chip, considering the anisotropic properties at the chip surfaces. Fig. 6 shows a schematical illustration of the three phases and their mass balances in the present mathematical model.

3. Case study: Delignification of Douglas fir softwood during kraft pulping

In this chapter, the proposed model is validated, and some remaining parameters are optimised based on the uniform pulping experiments at the cooking temperature of 130 °C by Ming [19]. The pulping experiments were designed to eliminate macro-scale influences such as non-uniform digester conditions and diffusion limitations within the porous system of the wood chip, focusing on the fibre scale phenomena during the kraft pulping process. An overview of the experiments and statistics for the fibre kappa number distribution is given in Table 1. Details of the experimental procedure are described in the thesis of Ming [19]. In the following, the skewness of the kappa number distribution will be neglected since it is close to zero. Therefore, the data follow a Gaussian distribution.

Kinetic and mass transfer models for the kraft pulping process are incorporated into the framework mentioned above. The remaining parameters are estimated to predict the experimental results from the Ming thesis.

The well-established kinetic model from the Purdue family is implemented with the reaction kinetics for the five solid and four liquid components. The solids consist lignin where 20% of lignin is high reactive (s_1) and 80% is low reactive (s_2), cellulose (s_3), galactoglucomanna (s_4) and xylan (s_5) [11]. The reaction rates for the solids in each concentration class are given by:

$$R_{s_i,n} = -e_f\left(k_{1,i}\rho_{e_1} + k_{2,i}\rho_{e_1}^{0.5}\rho_{e_2}^{0.5}\right)\left(\rho_{s_i,n} - \alpha_{s_i}^{\infty}\rho_{s_{i_0},n}\right) \tag{8}$$

where e_f is a constant effectiveness factor adjusting the reaction rate depending on the wood species, $\alpha_{s_i}^{\infty}$ represents the unreactive fraction of the solid component, $\rho_{s_{i_0},n}$ are the initial concentrations of each solid component in the respective concentration class, ρ_{e_1} and ρ_{e_2} are the effective alkali and hydrosulfide concentration in the entrapped liquor. The Arrhenius kinetic rate coefficients $k_{1,i}$*and* $k_{2,i}$ are calculated as:

$$k_{1,i} = A_{1,i}exp\left(\frac{-E_{1,i}}{RT}\right) \tag{9}$$

$$k_{2,i} = A_{2,i}exp\left(\frac{-E_{2,i}}{RT}\right) \tag{10}$$

Where R is the ideal gas constant, T is the temperature, $A_{1,i}$, $A_{2,i}$ are the pre-exponential factors and $E_{1,i}$, $E_{2,i}$ are the activation energies of the solid components. The reaction rates for the liquid components, active effective alkali (e_1), active hydrosulfide (e_2), dissolved lignin (e_3) and dissolved carbohydrates (e_4), are related to the total reaction rate of the solid components and the stoichiometric coefficient matrix b:

Table 3
Chemical composition of Douglas fir softwood (fraction of dry wood weight) [4].

Chemical component [-]	Fraction [-]	Average mass concentration [kg/m^3]
Lignin	0.293	155.29
Cellulose	0.388	205.64
Galactoglucomanna	0.175	92.75
Xylan	0.054	28.62
Extractives	0.053	28.09
Other polysaccharides	0.034	18.02

$$b = \begin{bmatrix} \beta_{OHL} - \frac{1}{2}\beta_{HSL} & \beta_{OHL} - \frac{1}{2}\beta_{HSL} & \beta_{OHC} & \beta_{OHC} & \beta_{OHC} \\ \frac{1}{2}\beta_{HSL} & \frac{1}{2}\beta_{HSL} & 0 & 0 & 0 \\ -1 & -1 & 0 & 0 & 0 \\ 0 & 0 & -1 & -1 & -1 \end{bmatrix} \quad (11)$$

An Arrhenius-type equation is used to predict the temperature dependency of the diffusion coefficients within the porous wood structure:

$$D_{direction} = D_{0,direction}\sqrt{T}e^{\frac{-E_{diffusion,\ direction}}{1.98T}} \quad (12)$$

with the pre-exponential constants $D_{0,direction}$ and activation energies $E_{diffusion,direction}$ presented by McKibbins [23]. Diffusion is assumed to be the same for all liquid components, although more rigorous diffusion models can be included in the present model framework [15,17,24]. The mass transfer at the boundary is calculated according to the film theory. Assuming that the external mass transfer from the bulk to the chip surface is negligible in a well-mixed digester, the mass transfer resistance is controlled by diffusion. The overall mass transfer coefficient reduced to:

$$K_{ol_{direction}} = \frac{D_{direction}}{\Delta direction} \quad (13)$$

where $\Delta direction$ refers to the distance between the chip surface and the chip centre of the respective coordinate, the structural changes of the wood chip are held constant in the model. Generally, this assumption might not be valid in a full-size kraft pulping digester where digester and chip-level limitation influence the mass transfer of the active chemicals, with additional mass transfer resistances. However, since the experiments were carried out to prevent non-uniform delignification as far as possible and assuming that the structural changes have a minor influence on the mass transfer in such an experimental setting, this assumption is justified. The porosity of the wood chips is calculated as:

$$\varepsilon = 1 - \frac{\rho_{wood}}{\rho_{solid}} \quad (14)$$

Table 4
Optimal values of the parameter optimisation.

Parameter	Value	Standard error
ϕ	0.588	0.048
$\sigma_{0,lignin}$	20.77	2.86

where ρ_{wood} is the density of the wood and ρ_{solid} is the density of the solid wood material. An overview of all used parameters is given in supplementary material.

The distribution of the Kappa number is calculated by the correlation [12]:

$$\kappa_n = \frac{\rho_{s_1,n} + \rho_{s_2,n}}{0.00153 \sum_{i=1}^{5}\rho_{s_i,n}} \quad (15)$$

In addition, the average yield for each chemical component is calculated as:

$$yield_i = \frac{\sum_{n=1}^{n}\rho_{s_i,average}}{\sum_{n=1}^{n}\rho_{s_{i_0},average}} \quad (16)$$

The literature provides qualitative evidence that the initial chemical compositions of solids are distributed over a concentration range across the wood chip, with knowledge about the fraction of the solids on the total wood [4,9]. However, quantitative measurements about the exact distribution are not available. Therefore, a Gaussian distribution for the concentration is assumed according to:

$$f(x) = \frac{1}{\sigma\sqrt{2\pi}}e^{-\frac{1}{2}\left(\frac{x-\mu}{\sigma}\right)^2} \quad (17)$$

with a mean concentration μ and a standard deviation of σ. As an initial starting point, the density of 530 $\frac{kg}{m^3}$ dry Douglas fir wood is chosen, assuming that the average density of one fibre is the same as for the wood (Table 3).

The standard deviations for the fundamental chemical components are unknown but can be deduced from the kappa number distribution data from Ming [19], using the model presented in this work.

Only the lignin standard derivation and one kinetic effectiveness factor are optimised against experimental data to keep the number of adjustable parameters as small as possible. The distributions of the other solid components follow directly from the lignin distribution, assuming that the overall chip density is constant. The reactions and distributions of the extractives and other polysaccharides are neglected in the model due to their rapid reaction and high liquid to wood ratio.

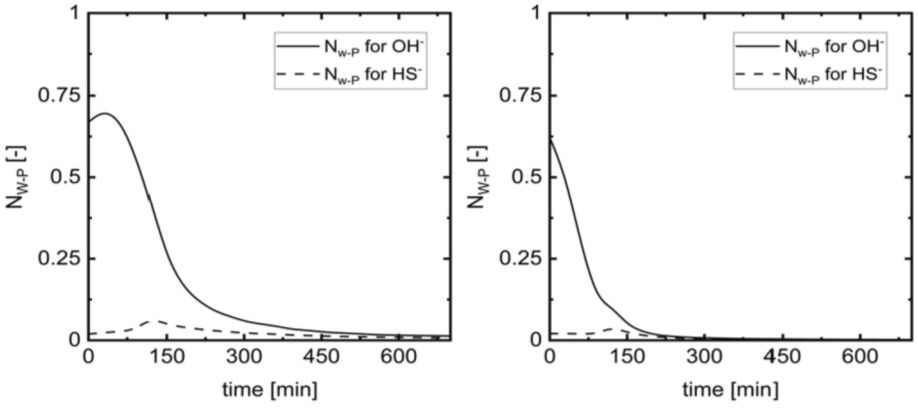

Fig. 7. Simulation of the Weisz-Prater criteria for the active chemicals in the experimental setup using effective alkali concentration 40 g/L (left) and 160 g/L (right) at 130 °C.

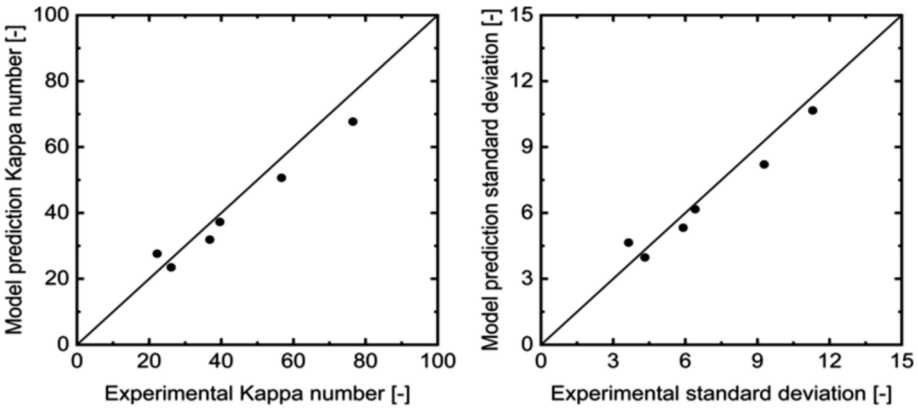

Fig. 8. Model predictions against experimental data for the average kappa number (left) and the standard deviation (right) of the fibre kappa number distribution.

4. Results and discussion

The cooking experiments carried out by Ming [19] are used to estimate the initial distribution of the lignin in the wood chip. Preliminary simulations with the average concentrations of the fundamental chemical components were conducted to assess the pore diffusion effect of the active chemicals on the reaction rates, using the Weisz-Prater criteria for a first-order reaction:

$$N_{W-P} = \frac{R_{volume,j} L^2}{\rho_j D_{eff}} \ll 1 \tag{18}$$

where $R_{volume,j}$ is the observed reaction rate of the active chemicals per volume wood chip, L is the characteristic length of the diffusion limiting direction, ρ_j are the concentrations of the active chemicals at the chip surface and D_{eff} is the effective diffusion coefficient [25]. The chip thickness is considered to be the diffusion limiting direction, and the effective diffusion coefficient includes the anisotropic properties for the thickness direction:

$$D_{eff,y} = D_y \frac{\varepsilon_{xz}}{\tau_{xz}} \tag{19}$$

As is shown in Fig. 7, the model predicts that the Weisz-Prater criterium holds for both initial effective alkali concentrations and active chemicals used in the experiments. Hence, the reaction rates of the active chemicals are not influenced by the diffusion rate to a level that would be significant at the present conditions. This is in accordance with the initial objective of the experimental setup and literature findings, which show that thin wood chips are less prone to experience non-uniform delignification due to diffusion limitations [26,27].

In the following, parameter optimisation for the effectiveness factor e_f and initial lignin standard deviation $\sigma_{0,lignin}$ are performed by solving the model with the "lsqnonlin" function provided in the MATLAB environment. A least-square objective function criterion for the kappa number average and standard deviation of the experimental data were used:

$$Q_{\kappa_{average}} = \left(\frac{\kappa_{average,model} - \kappa_{experiments}}{\kappa_{experiments}} \right)^2 \tag{20}$$

$$Q_{\sigma_\kappa} = \left(\frac{\sigma_{\kappa,model} - \sigma_{\kappa,experiments}}{\sigma_{\kappa,experiments}} \right)^2 \tag{21}$$

First attempts to optimise the parameters with one constant effectiveness factor for all fundamental chemical components resulted in an unsatisfied data fitting. Consequently, the adopted Purdue reaction rate expressions for the fundamental chemical components have to be adjusted, depending on the initial concentration of the effective alkali

Table 5
Model prediction and experimental results comparison of the statistics for the fibre kappa number distribution.

Pulp ID	Kappa number average		Standard deviation		COV	
	Measured	Model	Measured	Model	Measured	Model
EW01	76.5	68.2	11.3	10.63	0.15	0.156
EW02	56.7	51.1	9.28	8.2	0.16	0.16
EW03	36.8	32.3	5.91	5.35	0.16	0.165
EW04	26.1	23.9	4.32	4	0.17	0.168
HA01	39.6	37.7	6.41	6.18	0.16	0.164
HA02	22.2	28	3.64	4.67	0.16	0.167

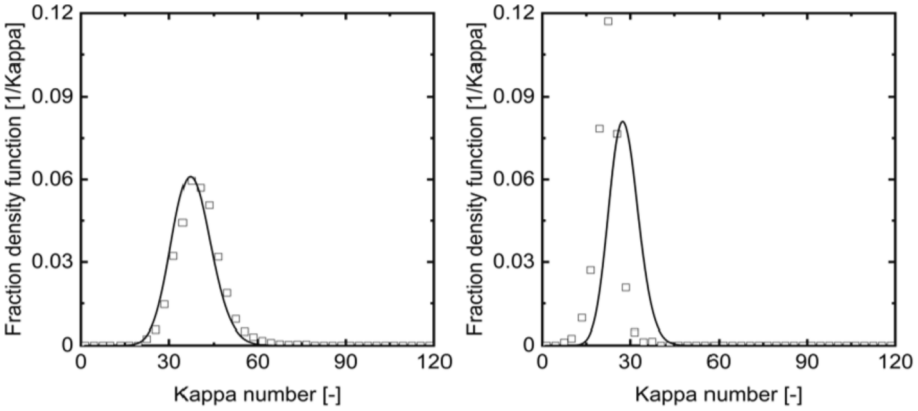

Fig. 9. Model predicted (solid) and experimental (scatter) fibre kappa number distribution for the cooking experiments using initial effective alkali concentration of 160 g/L, HA01 (left) and HA02 (right).

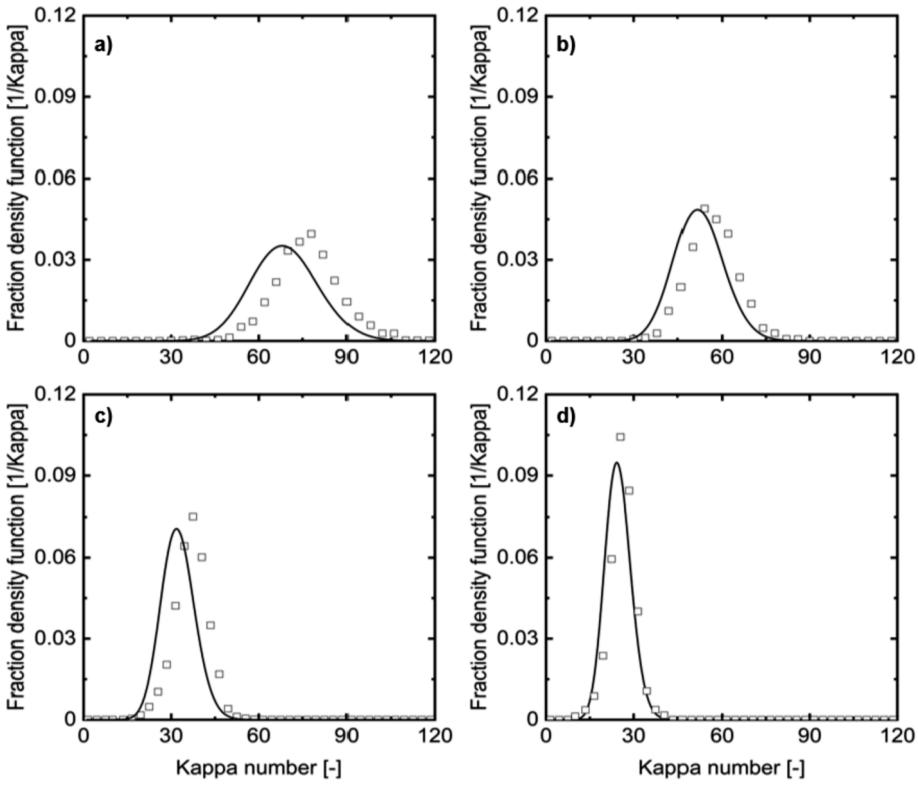

Fig. 10. Model predicted (solid) and experimental (scatter) fibre kappa number distribution for the cooking experiments using initial effective alkali concentration of 40 g/L, a) EW01, b) EW02, c) EW03, and d) EW04.

and/or the extent of the reaction.

Other researchers have also observed this dependency. Andersson et al. introduced a hybrid kinetic model between the Purdue and Washington University approach, using similar kinetic expression as the Purdue model family. The model distinguishes the fundamental chemical components into three different fractions of reactivity which depend on the prevailing process conditions (e.g., active chemicals and temperature) [28]. The model was able to predict the delignification of wood. However, the number of state variables raised from five in the original Purdue model to 12 in the Andersson model, making the kinetic expressions more complex and computational burden. An alternative kinetic model approach was proposed by Bogren et al. [29]. This kinetic model uses a continuous distribution of the lignin reactivity with a time-dependent rate constant, assuming an infinite number of different lignin reactivity fractions.

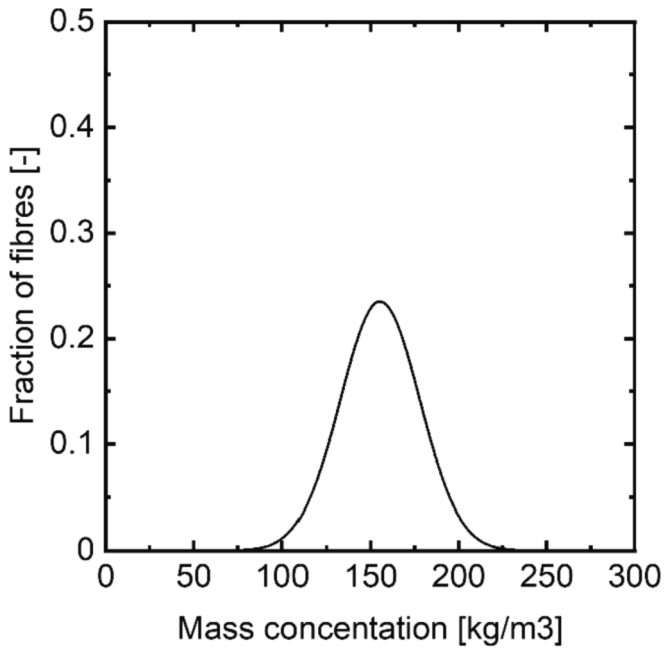

Fig. 11. Initial lignin distribution according to the presented model and parameter optimisation.

The present study proposes an extension of the Purdue kinetic expressions to account for a change in lignin reactivity during delignification. A yield-dependent effectiveness part expands the constant effectiveness factor of the Purdue model according to:

$$e_{fi} = e_{f0_i} yield_i^{\phi} \tag{22}$$

Where the effectiveness factor of the high and low reactive lignin has a constant, species-dependent reactivity part e_{f0_i} and a yield-dependent part with a parameter ϕ. Since the species-dependent reactivity part of Douglas fir is unknown, it is set to one. The reaction rates for the carbohydrates are the same as in the original Purdue kinetics, with a constant effectiveness factor also set to one. Hence, *eq. (22)* accounts for the chemical variation of lignin in different softwood species and the change in lignin reactivity during the pulping process, which originated from an alteration of lignin on a chemical structure level. The yield-dependent formulation was selected instead of time or other reactor type dependency to develop a model that can be applied in different digester types, including large scale continuous digester units.

The final optimised model parameters are the standard deviation of the initial lignin distribution and the factor ϕ for the yield-dependent effectiveness factors of the two lignin fractions. The optimisation is performed for all pulping experiments of both initial effective alkali concentrations, using 40 concentration classes in the model. Table 4 shows the optimal values for the parameters.

The cooking experiments data for the average kappa number and

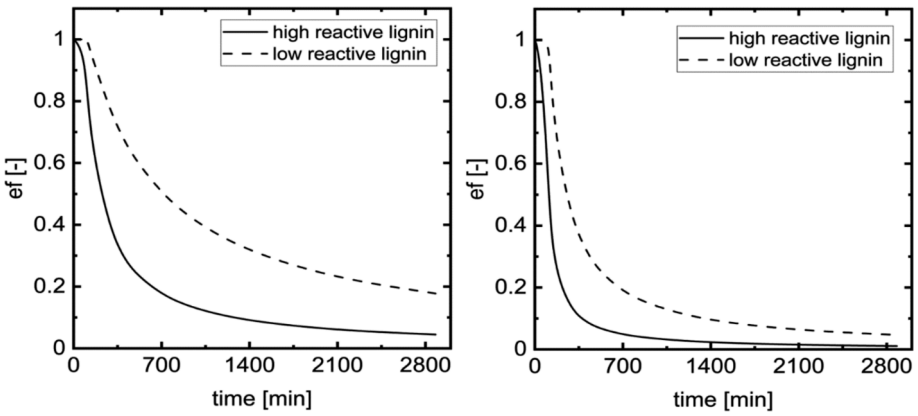

Fig. 12. Simulated decline of the effectiveness factor for the high and low reactive lignin. Initial concentration of 40 g/L effective alkali (left) and 160 g/L effective alkali (right) .

standard deviation are compared to the model prediction with the optimised parameters (Fig. 8 and Table 5). The model predicts the experimental data very well for all six cooking experiments.

Figs. 9 and 10 compare the exact shape of the kappa number distribution for both initial effective alkali cooking experiments. The model and experimental distributions are normalised by the kappa number class width for better comparison. Both sets of experiments are predicted reasonably well with the model, with some peak position and height discrepancies. However, these can be explained by normal experimental uncertainties and might be eliminated by a larger data set to average out the variances.

From the good agreement of the model and experimental kappa number distributions, an intrinsic fundamental chemical component distribution can be hypothesised as the origin of the observed kappa number distribution between individual fibres. This initial distribution can be related to the wood anatomy, where the fundamental chemical components are not uniformly distributed in the morphological regions and even within the same region, as is shown experimentally by Raman images [9]. Moreover, the lignin distribution is assumed to be similar in other softwood species than Douglas fir due to the rather subtle chemical structural variations across different softwood lignins [30]. Fig. 11 shows the initial lignin distribution according to the presented model and the parameter optimisation.

The model uses the widely accepted Purdue kinetic structure to evaluate the delignification of wood. However, the Purdue kinetics in their original form cannot predict the slowing down of the delignification and need to be adjusted by a yield-dependent lignin reaction. The simulated decline for the yield-dependent effectiveness factor of the

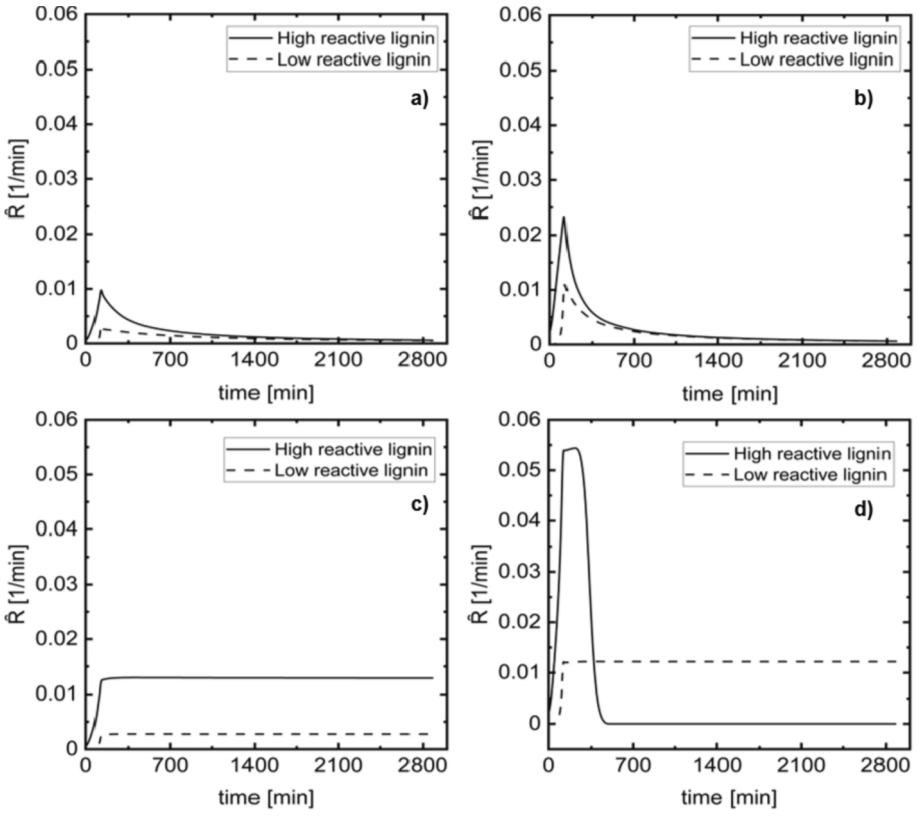

Fig. 13. Comparison of normalised reaction rates of the yield dependent lignin kinetics for a) EA 40 g/L, b) EA 160 g/L and original Purdue kinetics c) EA 40 g/L and d) 160 g/L.

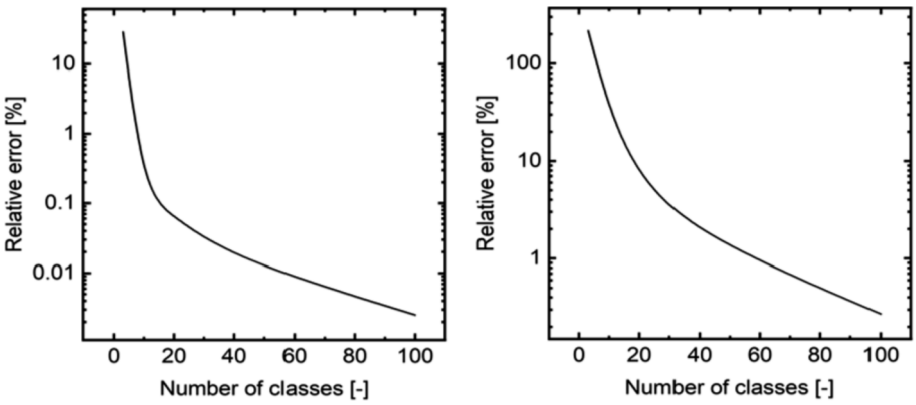

Fig. 14. Relative error for different concentration classes of the kappa number average (left) and the standard deviation (right) of the kappa number distribution prediction.

high and low reactive lignin are shown in Fig. 12.

In both cases of the initial active chemicals concentration, there is an immediate decrease in the effectiveness factor for the high reactive lignin. In contrast, the effectiveness factor for the low reactive lignin shows an offset until the cooking temperature is reached. This offset is an inherent effect of the original Purdue model, where the low reactive lignin does not react below a certain cooking temperature. The difference in the effectiveness factor between the initial concentrations is reflected in the rate of decline. For the milder cooking conditions with 40 g/L effective alkali, the decrease in the effectiveness factor is moderate compared to the abrupt decline in the case of the 160 g/L effective alkali. Moreover, the reactivity of lignin is higher towards the end of the cooking, in the case of the milder condition. Fig. 13 compares the original Purdue kinetic model with the proposed extension of the lignin kinetics. The reaction rates are normalised by the lignin concentrations predicted by the model and plotted against the pulping timespan. The original Purdue model shows an increase in reaction rate for both lignin fractions up to the point where the cooking temperature is reached and a constant reaction rate from that point. For the initial concentration of 160 g/L effective alkali, the reaction rate for the high reactive lignin decreases to zero at about 400 min as it becomes completely exhausted.

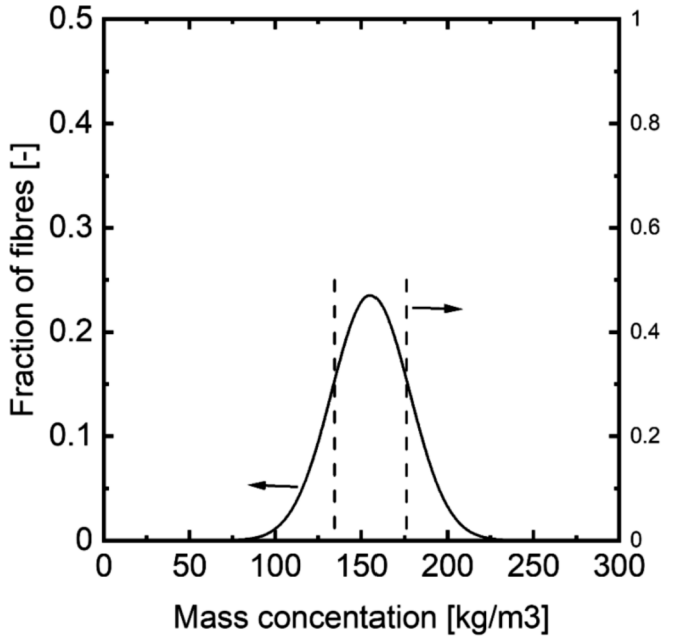

Fig. 15. Comparison of the 40 equal class (solid) and the two-class quadrature method of moments (vertical dash lines) for the lignin distribution.

In comparison, the yield-dependent extension of the reaction rates also increases up to the cooking temperature. However, the difference is that the reaction rates for both lignin fractions decrease throughout the reaction and converge to the same reaction rate towards the end of the cooking process.

The extension of the original kinetics provides a more realistic description of the progressive delignification of wood. One explanation for the decrease in reaction rate can be a continuous chemical change of the lignin towards a more resistant lignin structure during cooking. The qualitative change in the reaction predicted by the model is supported by experimental observations regarding the structural transformation of kraft lignin during delignification, which show that native lignin undergoes a chemical change throughout the kraft pulping process [31–33]. The origin of the different reactivity of lignin can be related to the morphological region in the wood. The lignin of the secondary wall has higher reactivity than the lignin of the middle lamella and the cell corner, as shown by topochemical studies [34,35]. The kinetics of the kraft pulping process are still the subject of ongoing research and an interesting topic of their own [36,37].

The investigations mentioned above were carried out for 40 equal size concentration classes to understand the phenomena and visualise the results in detail. However, 40 concentration classes can be computational heavy in a full-size digester model, including wood chip and digester level inhomogeneities. Therefore, the sensitivity of the results towards the number of discretisation classes is tested, and optimal positioning for the classes is proposed. Fig. 14 compares the relative error for the different number of concentration classes used in the simulation for equally distributed classes. The average kappa number is predicted well with concentration classes above 10. However, the standard deviation of the kappa number distribution needs at least 40 classes to be predicted within a reasonable relative error.

A second approach based on the product-difference algorithm [38] used for the solution of population balances with the quadrature method of moments [39] is tested to determine an optimal initial discretisation grid for the initial fundamental chemical components, based on the assumed density distribution for lignin. This approach can predict the average kappa number distribution and standard deviation with less than 0.25% relative error by using only two concentration classes. Fig. 15 compares the lignin distribution discretisation of the 40 equal classes and the two-class qmom method. With the optimised discretisation, a reasonably small number of additional variables is thus sufficient to capture the distributed nature of lignin around individual fibres. This helps to implement the present fibre distribution model into a full-scale digester model.

5. Conclusions

In this work, a novel mathematical approach for modelling lignocellulosic feedstock by considering the distributed character of the raw material was presented. The model was tested for Douglas fir softwood delignification. It is expected to predict the delignification of other softwoods due to the similarity in chemical structure across different softwood species. Parameters were optimised based on kraft pulping experiments, which were conducted to obtain the most uniform kappa number distribution for wood fibres. The cause of the non-uniform kappa number distribution can be assumed to be an inherent distribution phenomenon of the fundamental chemical components. Kinetic expressions from the Purdue kinetic model family were used to describe the delignification process. Initial attempts to optimise the wood species effectiveness factor proposed by the original Purdue kinetic model resulted in unsatisfactory model predictions. Therefore, an extension of the effectiveness factor was used, suggesting a change in lignin reactivity as the reaction progresses. The experimental kappa number distribution was well predicted with the introduced fundamental chemical component distribution across the wood fibres and the yield-dependent effectiveness for the reaction rates of lignin. The proposed model can easily be applied to systems where the reaction conditions vary, or the digester type is changed to a continuous digester. The model can be used for further studies regarding non-uniform delignification, which include inhomogeneities at the chip and digester level in addition to the heterogeneity at the fibre level.

Declaration of Competing Interest

The authors declare that they have no known competing financial interests or personal relationships that could have appeared to influence the work reported in this paper.

Acknowledgement

This work was financially supported and part of the Academy of Finland's Flagship Program under Projects No. 318890 and 318891 (Competence Center for Materials Bioeconomy, FinnCERES).

Appendix A. Supplementary data

Supplementary data to this article can be found online at https://doi.org/10.1016/j.cej.2022.135548.

References

[1] P.N. Ciesielski, M.B. Pecha, A.M. Lattanzi, V.S. Bharadwaj, M.F. Crowley, L. Bu, J. V. Vermaas, K.X. Steirer, M.F. Crowley, Advances in multiscale modeling of lignocellulosic biomass, ACS Sustain. Chem. Eng. 8 (9) (2020) 3512–3531, https://doi.org/10.1021/acssuschemeng.9b07415.
[2] K.L. Kenney, W.A. Smith, G.L. Gresham, T.L. Westover, Understanding biomass feedstock variability, Biofuels. 4 (1) (2013) 111–127, https://doi.org/10.4155/bfs.12.83.
[3] G. Mongkhonsiri, R. Gani, P. Malakul, S. Assabumrungrat, Integration of the biorefinery concept for the development of sustainable processes for pulp and paper industry, Comput. Chem. Eng. 119 (2018) 70–84, https://doi.org/10.1016/j.compchemeng.2018.07.019.
[4] H. Sixta, Handbook of Pulp, 2nd ed., WILEY-VCH Verlag GmbH & Co. KGaA, Weinheim, 2006.
[5] E. Sjöström, Wood Chemistry: Fundamentals and Applications, 2nd ed., Academic Press Inc., San Diego, 1993.
[6] J.A.N. Scott, A.R. Procter, B.J. Fergus, D.A.I. Goring, The application of ultraviolet microscopy to the distribution of lignin in wood description and validity of the technique, Wood Sci. Technol. 3 (1) (1969) 73–92, https://doi.org/10.1007/BF00349985.
[7] J.R. Wood, D.A.I. Goring, The distribution of lignin in stem wood and branch wood of Douglas fir, Pulp Pap. Mag. Can. 72 (1971) 61–68.
[8] S. Saka, R.J. Thomas, P. Science, N. Carolina, A study of lignification in loblolly pine tracheids by the SEM-EDXA Technique, Wood Sci. Technol. 179 (1982) 167–179, https://doi.org/10.1007/BF00353866.
[9] U.P. Agarwal, Raman imaging to investigate ultrastructure and composition of plant cell walls: Distribution of lignin and cellulose in black spruce wood (Picea mariana), Planta. 224 (5) (2006) 1141–1153, https://doi.org/10.1007/s00425-006-0295-z.
[10] C.C. Smith, Studies of the mathematical modelling, simulation, and control of the operation of a Kamyr continuous digester for the Kraft process, Purdue University, 1974.
[11] T. Christensen, A Mathematical model of the Kraft pulping process, Purdue University, 1982.
[12] P.A. Wisnewski, F.J. Doyle, F. Kayihan, Fundamental continuous-pulp-digester model for simulation and control, AIChE J. 43 (12) (1997) 3175–3192, https://doi.org/10.1002/aic.690431206.
[13] R.R. Gustafson, C.A. Sleicher, W.T. McKean, B.A. Finlayson, Theoretical model of the kraft pulping process, Ind. Eng. Chem. Process Des. Dev. 22 (1) (1983) 87–96, https://doi.org/10.1021/i200020a016.
[14] N. Agarwal, R. Gustafson, A contribution to the modeling of kraft pulping, Can. J. Chem. Eng. 75 (1) (1997) 8–15.
[15] J.P.F. Simão, A.P.V. Egas, M.G. Carvalho, C.M.S.G. Baptista, J.A.A.M. Castro, Heterogeneous studies in pulping of wood: Modelling mass transfer of alkali, Heterogeneous studies in pulping of wood: Modelling mass transfer of alkali 139 (3) (2008) 615–621, https://doi.org/10.1016/j.cej.2007.09.018.
[16] H. Grénman, J. Wärnå, J.-P. Mikkola, V. Sifontes, P. Fardim, D.Y. Murzin, T. Salmi, Modeling the influence of wood anisotropy and internal diffusion on delignification kinetics, Ind. Eng. Chem. Res. 49 (20) (2010) 9703–9711, https://doi.org/10.1021/ie101215a.
[17] J.P.F. Simão, M.G.V.S. Carvalho, C.M.S.G. Baptista, Heterogeneous studies in pulping of wood: Modelling mass transfer of dissolved lignin, Chem. Eng. J. 170 (1) (2011) 264–269, https://doi.org/10.1016/j.cej.2011.03.046.
[18] Z. Liu, V. Suntio, S. Kuitunen, J. Roininen, V. Alopaeus, Modeling of mass transfer and reactions in anisotropic biomass particles with reduced computational load, Ind. Eng. Chem. Res. 53 (10) (2014) 4096–4103, https://doi.org/10.1021/ie403400n.
[19] Q. Ming, Fundamental study of Kraft pulp Kappa uniformity, University of Washington, 2007.
[20] J. Tichy, A.R. Procter, M. Bloedel, Measurement and significance of lignin content uniformity in unbleached kraft pulps, Sven. Papperstidning. 84 (1981) R116-R119, R122.
[21] K. Hunt, J.V. Hatton, Determining the individial bleaching response of the components of a pulp mixture, Tappi J. 66 (1983) 103–104.
[22] P.O. Tikka, Conditions to extend Kraft cooking successfully. in, Pulping Conf, Boston, 1992.
[23] S.W. McKibbins, Application of diffusion theory to the washing of kraft cooked chips, Tappi J. 43 (1960) 801–805.
[24] S. Kuitunen, T. Vuorinen, V. Alopaeus, The role of Donnan effect in kraft cooking liquor impregnation and hot water extraction of wood, Holzforschung. 67 (2013) 511–521, https://doi.org/10.1515/hf-2012-0187.
[25] P.B. Weisz, C.D. Prater, Interpretation of measurements in experimental catalysis, Adv. Catal. 6 (1954) 143–196, https://doi.org/10.1016/S0360-0564(08)60390-9.
[26] J. Gullichsen, H. Kolehmainen, H. Sundqvist, On the nonuniformity of the kraft cook, Pap. Ja Puu - Pap. Timber. 74 (1993) 486–490.
[27] B.N. Hadler, W. Oniskot, The interdependence of chip thickness, cooking temperature and screenings in kraft cooking of pine, Sven. Papperstidning. 65 (1962) 905–910.
[28] N. Andersson, D.I. Wilson, U. Germgård, An improved kinetic model structure for softwood kraft cooking, Nord. Pulp Pap. Res. J. 18 (2003) 200–209, https://doi.org/10.3183/npprj-2003-18-02-p200-209.
[29] J. Bogren, H. Brelid, H. Theliander, Assessment of reaction kinetic models describing delignification fitted to well-defined kraft cooking data, Nord. Pulp Pap. Res. J. 23 (2008) 210–217, https://doi.org/10.3183/npprj-2008-23-02-p210-217.
[30] M. Balakshin, E.A. Capanema, X. Zhu, I. Sulaeva, A. Potthast, T. Rosenau, O. J. Rojas, Spruce milled wood lignin: Linear, branched or cross-linked? Green Chem. 22 (13) (2020) 3985–4001.
[31] P.M. Froass, A.J. Ragauskas, J.-e. Jiang, Chemical structure of residual lignin from kraft pulp, J. Wood Chem. Technol. 16 (4) (1996) 347–365, https://doi.org/10.1080/02773819608545820.
[32] G. Gellerstedt, K. Gustafsson, Structural changes in lignin during kraft cooking part 5. analysis of dissolved lignin by oxidative degradation, J. Wood Chem. Technol. 7 (1) (1987) 65–80, https://doi.org/10.1080/02773818708085253.
[33] C. Crestini, H. Lange, M. Sette, D.S. Argyropoulos, On the structure of softwood kraft lignin, Green Chem. 19 (17) (2017) 4104–4121.
[34] S. Saka, R.J. Thomas, J.S. Gratzl, D. Abson, S and Thomas, RJ and Gratzl, JS and Abson, Topochemistry of delignification in Douglas-fir wood with soda, soda-anthraquinone and karft pulping as determined by SEM-EDXA, Wood Sci. Technol. 16 (2) (1982) 139–153.
[35] D.G.P. Whiting, P., The topochemistry of delignification shown by pulping middle lamella and secondary wall tissue from black spruce wood, J. Wood Chem. Technol. 1 (1981) 111–122, https://doi.org/10.1080/02773818108085108.
[36] O. Fearon, S. Kuitunen, K. Ruuttunen, V. Alopaeus, T. Vuorinen, Detailed modeling of kraft pulping chemistry. delignification, Ind. Eng. Chem. Res. 59 (29) (2020) 12977–12985, https://doi.org/10.1021/acs.iecr.0c02110.
[37] O. Fearon, V. Nykänen, S. Kuitunen, K. Ruuttunen, R. Alén, V. Alopaeus, T. Vuorinen, Detailed modeling of the kraft pulping chemistry: carbohydrate reactions, AIChE J. 66 (2020) 1–9, https://doi.org/10.1002/aic.16252.
[38] R.G. Gordon, Error bounds in equilibrium statistical mechanics, J. Math. Phys. 9 (5) (1968) 655–663, https://doi.org/10.1063/1.1664624.
[39] R. McGraw, Description of aerosol dynamics by the quadrature method of moments, Aerosol Sci. Technol. 27 (2) (1997) 255–265, https://doi.org/10.1080/02786829708965471.